The Importance of Dendritic Mitochondria in the Morphogenesis and Plasticity of Spines and Synapses

Zheng Li,[1] Ken-Ichi Okamoto,[1]
Yasunori Hayashi,[1] and Morgan Sheng[1,2,*]
[1]The Picower Center for Learning and Memory
RIKEN-MIT Neuroscience Research Center
[2]Howard Hughes Medical Institute
Massachusetts Institute of Technology
Cambridge, Massachusetts 02139

Summary

The proper intracellular distribution of mitochondria is assumed to be critical for normal physiology of neuronal cells, but direct evidence for this idea is lacking. Extension or movement of mitochondria into dendritic protrusions correlates with the development and morphological plasticity of spines. Molecular manipulations of dynamin-like GTPases Drp1 and OPA1 that reduce dendritic mitochondria content lead to loss of synapses and dendritic spines, whereas increasing dendritic mitochondrial content or mitochondrial activity enhances the number and plasticity of spines and synapses. Thus, the dendritic distribution of mitochondria is essential and limiting for the support of synapses. Reciprocally, synaptic activity modulates the motility and fusion/fission balance of mitochondria and controls mitochondrial distribution in dendrites.

Introduction

Mitochondria are vital organelles present in all eukaryotic cells. In addition to carrying out aerobic respiration, mitochondria function actively in the buffering of intracellular Ca^{2+} and in the mechanisms of apoptosis. Mitochondria usually exist as tubules of variable size that fuse, divide, and branch in a dynamic reticular network (Karbowski and Youle, 2003; Yaffe, 1999). Individual mitochondria can also move within the cytoplasm, thus allowing them to distribute within cells and to partition between dividing cells (Yaffe, 1999).

The fission and fusion of mitochondria is regulated by large GTPases of the dynamin family, in particular, Drp1 (dynamin-related protein-1) and OPA1 (optic atrophy1) (Westermann, 2002; Yoon and McNiven, 2001). Drp1, a primarily cytoplasmic protein, regulates mitochondrial morphology and distribution but apparently does not affect the transport functions of the secretory and endocytic pathways (Pitts et al., 1999; Smirnova et al., 1998). OPA1 protein is located in mitochondria (Olichon et al., 2002). Mutation of the OPA1 gene causes the most common form of hereditary optic atrophy (Delettre et al., 2002). By regulating mitochondrial fission/fusion, Drp1 and OPA1 control the morphology and distribution of mitochondria (Misaka et al., 2002; Olichon et al., 2003; Yaffe, 1999). Dominant-negative mutants of Drp1 inhibit mitochondrial division, cause aggregation

*Correspondence: msheng@mit.edu

of mitochondria in the perinuclear region of cultured cells (Smirnova et al., 1998, 2001), and protect cells from apoptosis (Frank et al., 2001). To date, OPA1 and Drp1 functions have been studied only in nonneuronal cells, and their effects on neuronal mitochondria are unknown.

It is generally believed that the intracellular distribution of mitochondria is adapted to cellular physiology. However, the functional significance of proper mitochondrial distribution within cells is largely unknown. This may be because experimental perturbations of mitochondrial distribution are usually performed in cell lines with low morphological complexity, in which the consequences of improper mitochondrial targeting are difficult to assess. Neurons, on the other hand, are elongated cells with multiple compartments (e.g., dendrites, axons, and synapses) that are located far from the cell body. It should be easier to determine the effects of defective mitochondrial distribution in neurons, because certain cellular functions, such as synaptic transmission and plasticity, are mediated by distant subdomains that can become isolated from their nearest mitochondria.

The local need for ATP and Ca^{2+} handling is especially great at synapses, and mitochondria are frequently found in axon terminals (Rowland et al., 2000; Shepherd and Harris, 1998). In the *Drosophila* mutant Milton, defective synaptic transmission is associated with the loss of mitochondria from axon terminals (Stowers et al., 2002), supporting the functional importance of presynaptically targeted mitochondria. On the postsynaptic side, however, little is known about the importance of proper mitochondrial distribution in dendrites. In contrast to the abundance of mitochondria in presynaptic terminals, mitochondria are rarely found in dendritic spines (Adams and Jones, 1982; Cameron et al., 1991; Chicurel and Harris, 1992), the postsynaptic compartment of most excitatory synapses.

Mitochondria are believed to concentrate in subcellular regions with high metabolic requirements. For instance, they accumulate in the vicinity of active growth cones of developing neurons (Morris and Hollenbeck, 1993). However, whether or how this subcellular distribution is regulated by neuronal activity is unknown.

To address these questions, we investigated the distribution of mitochondria in dendrites of living hippocampal neurons. Our studies reveal that mitochondria dynamically redistribute into dendritic protrusions in response to synaptic excitation and correlated with synaptogenesis and spine formation. The dendritic distribution of mitochondria, which is regulated by Drp1, OPA1, and neuronal activity, appears to be an essential and limiting factor for synapse density and plasticity.

Results

Morphology and Distribution of Dendritic Mitochondria in Cultured Hippocampal Neurons

We used time-lapse confocal microscopy to study the distribution and movement of mitochondria labeled with "MitoDsRed" (DsRed2 fused to the mitochondrial tar-

geting sequence of cytochrome c oxidase [Rizzuto et al., 1995]). An enhanced variant of YFP ("Venus" [Nagai et al., 2002]) was cotransfected to visualize neuronal morphology. Hippocampal neurons were transfected at 12 or 14 days in vitro (Div12/14) and examined 2–3 days later. As visualized by MitoDsRed, mitochondria in hippocampal neurons were globular or tubular in shape and highly variable in size (see Supplemental Figures S1B and S1E at http://www.cell.com/cgi/content/full/119/6/873/DC1/). Most dendritic mitochondria were <5 μm in length (average 2.3 μm). A small proportion of dendritic mitochondria appeared extremely long (>10 μm, 2.6% of 230 mitochondria). The length of dendritic mitochondria measured by MitoDsRed confocal microscopy is similar to that of dendritic mitochondria in the brain measured by electron tomography (Perkins et al., 2001).

Mitochondria were abundant and overlapping in soma and large-diameter proximal dendrites but were separate from each other in small-diameter dendrites and distal dendrites (see Supplemental Figures S1B and S1E on the *Cell* web site). In dendrites 20–100 μm away from the soma, the mean dendritic mitochondrial index (ratio of total mitochondrial length in the dendritic shaft to dendritic length in a given dendritic segment) was 0.47 $\pm$ 0.015. More than 90% of dendritic mitochondria is confined to the shaft of the dendrite. Mitochondria in dendritic protrusions (defined as projections from the dendritic shaft of 0.5–5 μm in length, with or without an enlarged tip, thus including both dendritic spines and filopodia) were rarely observed in mature neurons (older than Div18).

To quantify mitochondrial motility in dendrites, we collected dual wavelength confocal images of neurons transfected with MitoDsRed and Venus every 3 s (see Experimental Procedures). Dendritic mitochondria 20–50 μm from the soma were selected for time-lapse imaging; their average speed was 0.39 $\pm$ 0.031 μm/min.

Developmental Change in Mitochondrial Distribution

We observed that a minority (<10%) of dendritic protrusions (dendritic spines and filopodia) contained mitochondria. Two kinds of mitochondria were associated with dendritic protrusions: small vesicular mitochondria (diameter <1 μm) that were entirely enclosed within protrusions (top three rows of Figure 1A) and larger-shaft mitochondria, part of which extended into protrusions (bottom three rows of Figure 1A).

We quantified the fraction of mitochondria that were present in dendritic protrusions, counting mitochondria in dendritic segments 20–100 μm from the soma. At Div11 and Div14, during an active period of synaptogenesis and spine development in culture, $\sim$8%–9% of mitochondria were at least partially in dendritic protrusions (Figure 1B). At Div18, this fraction fell to $\sim$4%. Infiltrating mitochondria showed no preference for a specific type of dendritic protrusion, such as large spines or thin filopodia. The fraction of dendritic protrusions that contained mitochondria also decreased with development (Figure 1C). The temporal coincidence of increased mitochondrial incursion into dendritic protrusions with a period of active spine/synapse formation suggests a possible relationship between mitochondrial function and spine/synapse development.

Repetitive Depolarization Increases Mitochondria in Dendritic Protrusions

Might mitochondria also be associated with the formation of dendritic protrusions accompanying morphological plasticity of neurons? We used time-lapse microscopy to examine mitochondrial distribution in the same hippocampal neurons before and after repetitive depolarization with 90 mM KCl (4 $\times$ KCl). New filopodia and dendritic spines as well as morphological changes of existing protrusions were observed in response to repeated depolarization, as reported previously (Wu et al., 2001). Strikingly, dendritic mitochondria were also redistributed to dendritic protrusions by 4 $\times$ KCl (Figures 2A–2I, arrowheads). Before stimulation, 8.3% $\pm$ 1.3% of dendritic mitochondria was in dendritic protrusions, but this number increased to 21.5% $\pm$ 5.2% at 3 hr after stimulation (Figure 2V). The number of dendritic protrusions that contained mitochondria was also increased by 4 $\times$ KCl (Figure 2W).

More detailed time-lapse imaging revealed that mitochondria typically first changed their shape during 4 $\times$ KCl stimulation (Figures 2J–2M). Mitochondria tended to change from elongated structures to more aggregated clusters, usually located around the base of the dendritic protrusion into which mitochondria moved (Figures 2J–2O, 2P, and 2S). Perhaps as a result of this, the dendritic mitochondrial index was reduced by 4 $\times$ KCl stimulation (Figure 2X), in contrast to the increase of mitochondria in dendritic protrusions. By 1 hr after the repetitive depolarization, mitochondria projected branches sideways (Figure 2N, arrowheads). The mitochondrial branches that extended out of the dendritic shaft colocalized with dendritic protrusions (Figures 2P–2U, arrowhead). Mitochondrial extensions into dendritic protrusions varied from $\sim$0.5–2 μm in length and from $\sim$1 hr to >6 hr in lifetime.

Local Synaptic Stimulation Induces Mitochondrial Extension into Dendritic Protrusions

We also examined whether synaptic stimulation can affect mitochondrial distribution in organotypic hippocampal slice cultures. Dendrites and mitochondria of CA1 pyramidal neurons were visualized by cotransfected GFP and MitoDsRed. Electrical stimulation was applied through a glass electrode placed 5–20 μm from the labeled dendrite to activate presynaptic inputs (Figure 3A). Two dendritic segments of the same neuron were monitored by time-lapse two-photon microscopy, one close to the stimulation electrode (Figure 3A, region a) and the other $\sim$100 μm away (region b). Tetanic stimulation (100 Hz for 1 s) induced the enlargement of a subset of spines within 2 min in the stimulated but not the unstimulated region (Matsuzaki et al., 2004; Okamoto et al., 2004). Specifically in the stimulated region, dendritic mitochondria showed morphological changes. In particular, they often collected in large bright globules subjacent to the enlarged spines (Figure 3C), suggesting mitochondrial recruitment to the immediate vicinity of active synapses. In the stimulated region of the dendrite, the mitochondrial index fell significantly (Figure 3D; dendritic mitochondrial index was measured within 5 μm distance of enlarged spines), as did average mitochon-

A Venus MitoDsRed Merge

2 μm

B **C**
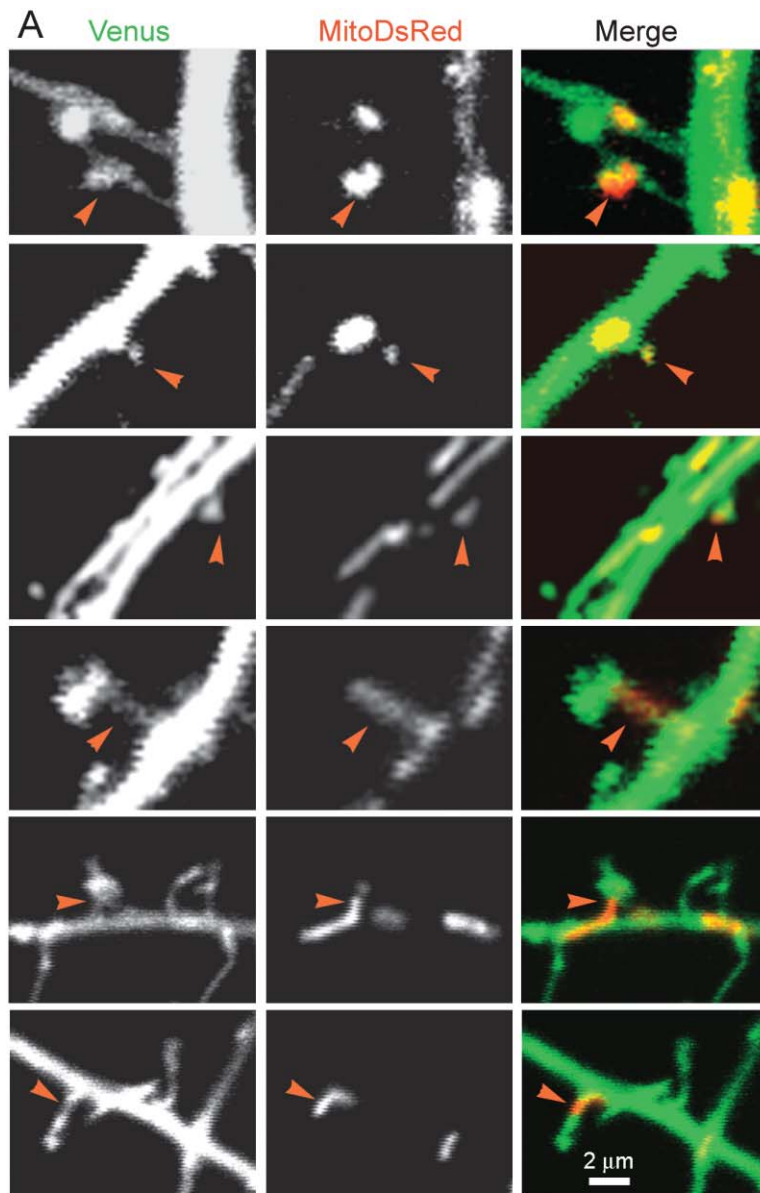
Figure 1. Localization of Mitochondria in Dendritic Protrusions and Its Regulation during Development

Hippocampal neurons were transfected with MitoDsRed and Venus and imaged 2–3 days after transfection. (A) Examples of dendritic protrusions that contain mitochondria. Arrowheads indicate mitochondria that are enclosed in protrusions (top three rows) or extend into protrusions from the dendritic shaft (bottom three rows). (B) Quantitation of the percentage of dendritic mitochondria (mean ± SEM) that are present in protrusions at different ages in culture. (C) Percent of protrusions (mean ± SEM) containing mitochondria at different ages in culture. n = 10–15 neurons for each age of neurons. **$p < 0.01$, Student's t test.

drial length (6.23 ± 2.32 μm before stimulation, 2.32 ± 0.73 μm after stimulation; p = 0.05).

As soon as 30 min following tetanic stimulation, extension of mitochondria into spines was observed in the dendritic region close to the stimulating electrode (four out of five stimulated cells). The mean percentage of spines containing mitochondria increased from ∼5% before stimulation to ∼19% after stimulation in region a (Figure 3E). The penetration of mitochondria into dendritic spines persisted for at least 90 min after tetanus (Figure 3C). There was no change in mitochondrial distribution in region b. The NMDA receptor antagonist APV
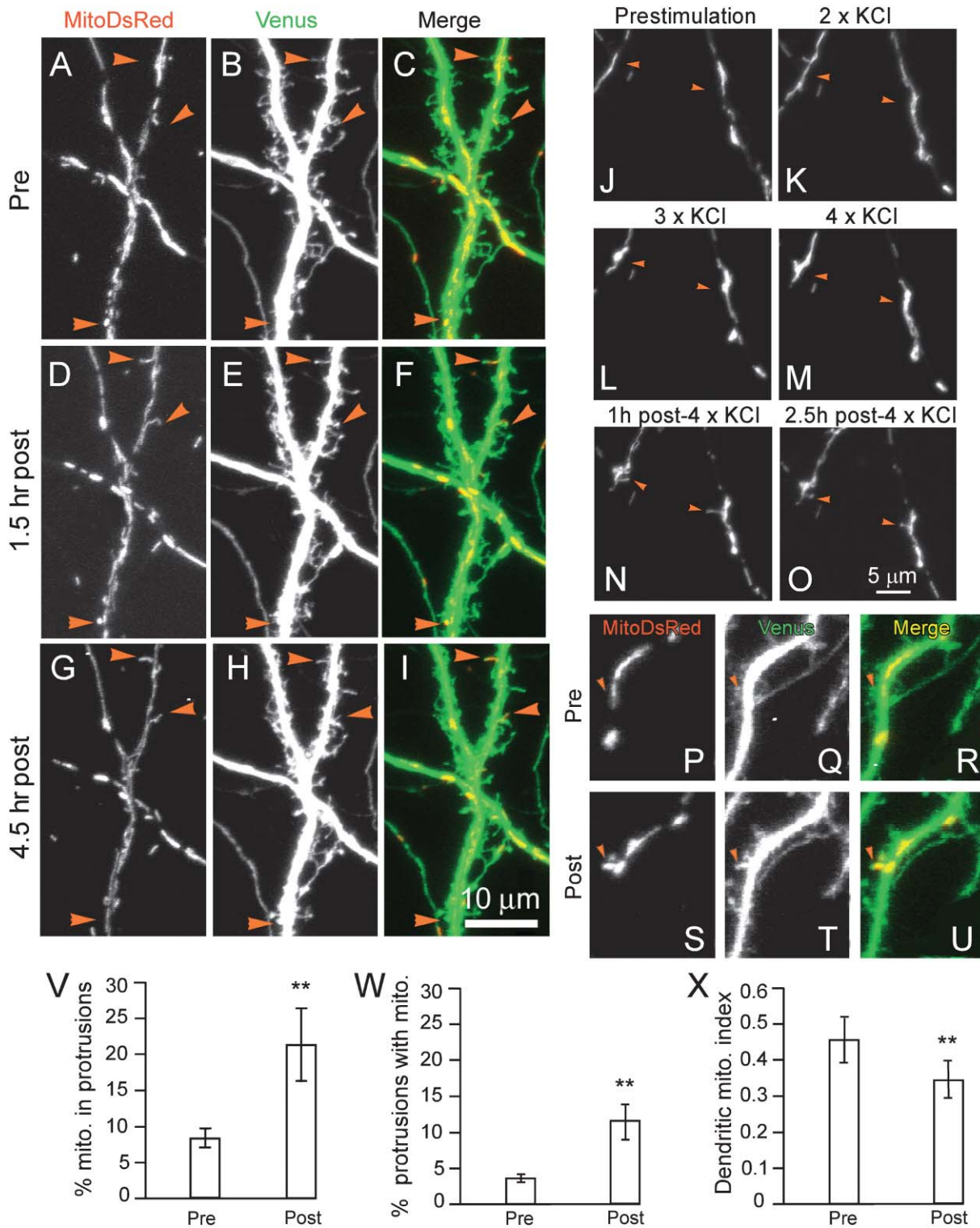
Figure 2. Repetitive Depolarizing Stimulation Induces Redistribution of Mitochondria into Dendritic Protrusions

Div14 neurons transfected with MitoDsRed and Venus were stimulated four times with 90 mM KCl (3 min exposure with 10 min intervals). The same neuron was dually imaged for Venus and MitoDsRed before (pre), during, and at various times after (post) 4 × KCl stimulation. (A–I) Time-lapse images showing examples (arrowheads) of mitochondria that extend into dendritic protrusions following stimulation. (J–O) Higher magnification view of dendritic mitochondria before, during, and after 4 × KCl. Arrowheads indicate mitochondria that change morphology during the stimulation and project a side branch after stimulation. (P–U) A dendritic segment showing an example of a dendritic protrusion that acquires a mitochondrion following 4 × KCl stimulation (arrowhead). (V) Quantitation of the percent of mitochondria in dendritic protrusions before and after 4 × KCl stimulation. (W) Percent of protrusions containing mitochondria before and after 4 × KCl stimulation. (X) Dendritic mitochondrial index before and after 4 × KCl stimulation. n = 13 neurons, **p < 0.005, Student's t test.

blocked the extension of mitochondria into dendritic spines (Figure 3E), implying that mitochondrial redistribution was due to synaptic excitation.

Effects of Drp1 and OPA1 on Dendritic Mitochondrial Distribution

The above experiments indicate that mitochondria redistribute toward dendritic protrusions in response to synaptic stimulation and during morphological development and plasticity of spines. Is the proper distribution of mitochondria important for spine development and/or maintenance? To address this question, we altered mitochondrial distribution and morphology in neurons by overexpression of wild-type and dominant-negative mutants of Drp1 and OPA1.

In hippocampal neurons transfected with dominant-negative Drp1 (Drp1-K38A, mutated in its GTPase domain [Smirnova et al., 1998]), dendrites were clearly depleted of mitochondria (Figure 4H). The dendritic mitochondrial index was reduced ∼40% (Figure 4V). Conversely, overexpression of wild-type Drp1 strongly increased the density of mitochondria in dendrites (compare Figures 4E and 4B), and the dendritic mitochondrial index increased by ∼50% (Figure 4V). The amount of mitochondria in the cell body (quantified as cumulative mitochondria area/cell body area) was slightly reduced by Drp1-K38A (5.40 ± 0.23 versus 6.45 ± 0.27 in control cells) and not significantly affected by wild-type Drp1 overexpression (6.65 ± 0.32). Thus, Drp1 is critical for distribution of mitochondria to dendrites, possibly by facilitating mitochondrial fission in the neuronal soma.

Overexpression of Drp1 or Drp1-K38A had no effect on the distribution of ER and Golgi, which were found to concentrate in the cell body and extend into dendrites (Supplemental Figure S2). The distribution and motility of endo-GFP-labeled endosomes, and NMDA-induced internalization of AMPA receptor subunit GluR2, were unaffected by Drp1 or Drp1-K38A (Supplemental Figures S3A and S3B). Thus, the effects of Drp1 overexpression or dominant-negative mutant appear to be relatively specific for mitochondria.

Overexpression of OPA1 in cultured cell lines causes fragmentation of mitochondria, altering morphology from tubular to vesicular (Misaka et al., 2002). We found that overexpression of wild-type OPA1 in hippocampal neurons had little effect on the number of mitochondria in dendrites (2.0 mitochondria/10 μm in OPA1 cells versus 2.1 mitochondria/10 μm in control cells), but the average length of dendritic mitochondria was reduced by ∼30% (1.62 ± 0.020 μm for OPA1-transfected neurons, 2.30 ± 0.020 μm for control; p = 0.002). This resulted in a reduced dendritic mitochondrial index (Figures 4K and 4V).

Effects of Drp1 and OPA1 on Dendritic Spines and Synapses

To assess the effect of Drp1 and OPA1 on dendritic spines, neurons were cotransfected with Venus to outline dendritic morphology. Transfection with Drp1 or OPA1 constructs was not overtly toxic to neurons over the several days' duration of our experiments and did not affect the pattern of arborization of dendrites. Dendritic spines were defined as protrusions of 0.5–5 μm in length

that had a clear neck and expanded tip (head) or a stubby shape. In neurons transfected with dominant-negative Drp1 or wild-type OPA1, the density of dendritic spines decreased by 79% and 54%, respectively (Figures 4G, 4J, and 4W). Remarkably, overexpression of wild-type Drp1 had the opposite effect, increasing the density of dendritic spines almost 2-fold (Figures 4D and 4W). Therefore, the density of dendritic spines correlates with the dendritic mitochondria index.

Drp1 had similar effects on mitochondria and dendritic spines in organotypic hippocampal slice cultures. In dendrites (200–400 μm from the soma) of CA1 pyramidal neurons, the dendritic mitochondrial index and spine density were increased by transfection with wild-type Drp1 and decreased by Drp1-K38A (Figures 4M–4U, 4X, 4Y).

Dendritic spines reflect excitatory synapses. To examine whether Drp1 also affects synapse number, we stained cultured hippocampal neurons for PSD-95, a marker for excitatory synapses. The density of PSD-95 puncta was increased by overexpression of wild-type Drp1 but decreased by Drp1-K38A or OPA1 (Supplemental Figures S4A and S4C). From these data, we conclude that the density of spines/synapses is influenced by GTPases that regulate mitochondrial fission and distribution.

Functional presynaptic boutons were visualized by uptake of styryl dye FM 4-64. The density of FM dye-labeled puncta on transfected cells was increased by overexpression of wild-type Drp1 but reduced by Drp1-K38A or OPA1 (Supplemental Figures S4B and S4D). Thus, the promoting effect of Drp1 on the density of postsynaptic specializations was associated with an increased number of functional presynaptic terminals made on the transfected cell.

Taken together, these findings indicate that Drp1 and OPA1 are important for development and/or maintenance of spines and synapses. Since Drp1 is believed to act specifically on mitochondrial fission and distribution (see above and Smirnova et al. [1998]) and OPA1 is a protein specifically targeted to mitochondria (Misaka et al., 2002; Olichon et al., 2002), the effects of these GTPases on neuronal synapses are most likely mediated by their effects on the morphology and distribution of mitochondria. The surprising finding that overexpression of Drp1 increases the density of spines and synapses implies that mitochondria are not only required but limiting for the formation and/or maintenance of synapses.

Creatine Mimics the Effect of Drp1 on Synapse Density

If the promoting effect of Drp1 on synapse density is due to increased dendritic mitochondria, we reasoned that pharmacological enhancement of mitochondrial function might have a similar effect. Hippocampal neurons were treated with 20 mM creatine, which is reported to stimulate mitochondrial respiration (Walsh et al., 2001). Mitochondrial function was assessed by staining with the lipophilic cationic dye JC-1 (5,5′,6,6′-tetrachloro-1,1′,3,3′-tetraethylbenzimidazol-carbocyanine iodide). At low concentrations in mitochondria, JC-1 exists as monomers (emission peak 527 nm; green fluores-
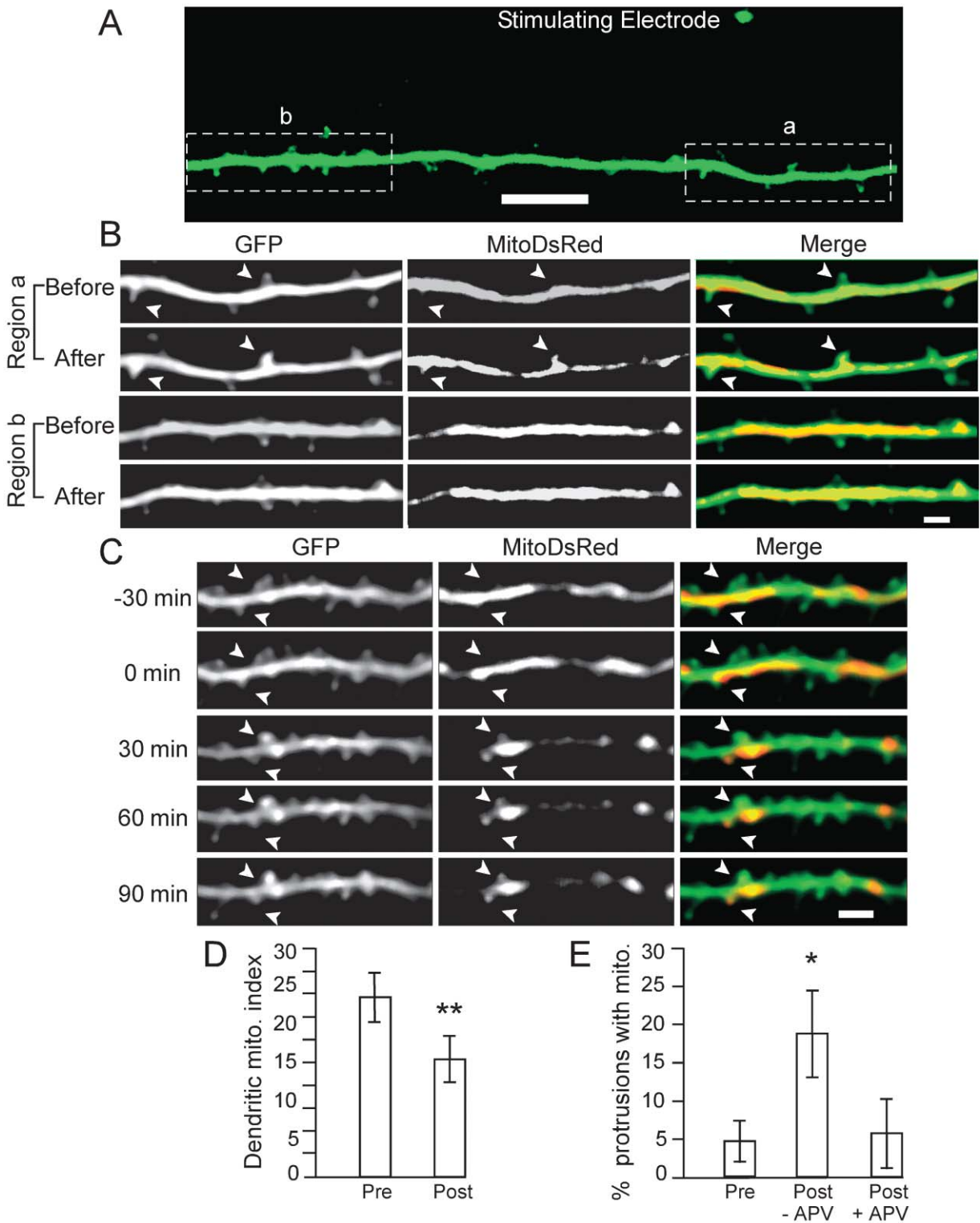
Figure 3. Local Synaptic Stimulation in Cultured Hippocampal Slices Redistributes Mitochondria into Dendritic Spines

CA1 pyramidal neurons of hippocampal slice cultures (1–2 weeks in culture) were transfected with GFP and MitoDsRed. (A) Example of a transfected dendrite, showing location of stimulating electrode (green spot). Regions "a" and "b" are indicated. (B) Dendritic region a (closest to stimulating electrode) and region b (~100 μm away from the electrode) were imaged for GFP and MitoDsRed before and 30 min after tetanic stimulation (100 Hz, 1 s). Mitchondrial translocation into enlarged dendritic protrusions was observed in the stimulated region (region a, arrowheads) but not in distant part of the same dendrite (region b). (C) Time-lapse images of GFP and MitoDsRed in a dendritic segment captured at 30 min intervals before and after tetanic stimulation (stimulation was applied at 0 min). Mitochondrial penetration into enlarged spines (arrowheads) was observed 30 min after stimulation and persisted until the end of observation (90 min). Scale bar, 10 μm for (A),

cence). At higher concentrations, JC-1 forms aggregates in mitochondria (emission peak 590 nm; red). Because JC-1 accumulates to a higher concentration in mitochondria with higher membrane potentials, the ratio of red/green fluorescence of JC-1 can be used as an indicator of mitochondrial function (Smiley et al., 1991).

Treatment with 20 mM creatine for 12 hr dramatically increased the red/green ratio of JC-1 staining (Figures 5A–5F and 5K), confirming that creatine stimulated mitochondrial activity. As with Drp1 overexpression, creatine treatment (12 hr) increased the density of endogenous PSD-95 clusters and the integrated intensity of PSD-95 immunofluorescence per dendrite length (Figures 5G–5J and 5L). Thus, pharmacological enhancement of mitochondrial function also promotes synapse density.

Drp1 and Creatine Promote Activity-Dependent Synaptogenesis

Do mitochondria also play a role in activity-dependent morphological plasticity of spines/synapses? Repeated depolarization (90 mM KCl) activates the Ras-MAP kinase pathway and induces the formation of dendritic protrusions (Wu et al., 2001). We found that repeated spaced K$^+$ depolarizations (4 × KCl) induced the formation of new synapses in cultured hippocampal neurons (Figure 6). Neurons were cotransfected with PSD-95-Venus to label excitatory synapses and MitoDsRed to label mitochondria, and the same cells were imaged by time-lapse microscopy before and 9 hr following 4 × KCl stimulation. 4 × KCl increased the density of PSD-95-Venus puncta by ∼40% (Figures 6A–6D and 6Q), indicating a net increase of synapse number over 9 hr. In neurons that were additionally transfected with Drp1, 4 × KCl induced an even larger increase in PSD-95-Venus puncta (∼100% increase in density; Figures 6E–6H and 6Q). Thus, not only does Drp1 increase the steady-state density of spines/synapses (see Figure 4), it also promotes the synaptogenic response to potentiating stimuli. Conversely, Drp1-K38A blocked the increase of PSD-95-Venus puncta induced by 4 × KCl (Figures 6M–6P and 6Q). In summary, synapse formation was enhanced by Drp1 overexpression, which increased the dendritic mitochondrial index, and inhibited by dominant-negative Drp1, which decreased the dendritic mitochondrial index.

Neurons treated with creatine (20 mM) also showed a greater increase of PSD-95-Venus puncta density than did control cells after 4 × KCl stimulation (Figures 6I–6L and 6Q). Thus, enhanced mitochondrial function potentiated the synaptogenic response to repeated depolarization similarly to Drp1 overexpression, supporting the idea that mitochondrial function is limiting for synaptogenesis.

Effect of Activity on Motility and Balance of Fusion and Fission of Dendritic Mitochondria

The effect of neuronal activity on mitochondrial distribution and motility has not been directly examined in dendrites or axons. To manipulate global activity levels in culture, we treated hippocampal neurons with 1 μM tetrodotoxin (TTX) to block action potentials or 50 mM KCl to depolarize neurons. Up to 4 hr exposure to 50 mM KCl did not cause excitotoxicity of neurons, as measured by propodium iodide staining (data not shown).

Prior to drug treatment (baseline), the speed of mitochondrial movement ranged from 0.10 to 0.70 μm/min (mean 0.39 ± 0.031 μm/min) (Figures 7A and B). The rate of mitochondria movement was increased by TTX but reduced by KCl depolarization (Figures 7A and 7B). Thus, increased activity is associated with reduced mitochondrial motility, whereas depressed activity is correlated with increased mitochondrial motility.

The effect of 50 mM KCl was largely prevented by 10 μM nimodipine or 100 μM DL-APV (Figure 7B), indicating that Ca^{2+} influx through L-type Ca^{2+} channels and/or NMDA receptors mediates the dampening effect of depolarization on mitochondrial movement. Transfection with Drp1-K38A did not affect the "basal" motility of mitochondria (0.30 ± 0.064 μm/min in Drp1-K38A-transfected neurons versus 0.39 ± 0.031 μm/min in control cells, p = 0.33), but it abolished the change of mitochondrial motility induced by TTX or 50 mM KCl (Figure 7B). This result suggests that Drp1 is required for activity-dependent regulation of mitochondrial movement.

Time-lapse imaging of mitochondria during 4 × KCl depolarization showed changes in mitochondrial morphology that were suggestive of regulated fusion and/or fission (Figures 2J–2O). To analyze this in more detail, we measured mitochondrial fusion/fission by time-lapse imaging of hippocampal neurons transfected with MitoDsRed and Venus. Dendritic mitochondria 20–100 μm from the cell body were imaged every 5 min. A fusion event was defined as the physical connection of two or more mitochondria, following which the fused mitochondrion stayed intact and moved together for ≥10 min. Mitochondrial fission was recognized by the separation of a single mitochondrion into two or more distinct mitochondria. The ratio of fusion/fission was quantified to control for variability in mitochondrial density in different dendrite segments.

Overexpression of wild-type Drp1 decreased the ratio of mitochondrial fusion/fission, whereas dominant-negative Drp1 increased it (Figure 7D). This is consistent with the general view of Drp1 as a fission protein. To analyze the influence of activity, the mitochondrial fusion/fission ratio was measured in the same neuron before and within 2 hr after treatment with 1 μM TTX or 50 mM KCl. In control neurons, TTX raised the mean mitochondrial fusion/fission ratio by 4.5-fold (Figure 7E). In contrast, K$^+$ depolarization reduced the fusion/fission ratio by 57% (Figure 7F). Thus, the balance of mitochondrial fusion/fission is shifted toward fusion in "silenced" neurons and toward fission in depolarized neurons. In Drp1-transfected neurons, the mitochondrial fusion/fission ratio still increased in the presence of TTX but to a lesser extent (Figure 7G). However, 50 mM KCl failed

---

2 μm for (B) and (C). (D) Dendritic mitochondrial index (measured within 5 μm distance of spines enlarged after tetanic stimulation) in dendritic region a before and after tetanic stimulation. (E) Percent of spines containing mitochondria before and after tetanic stimulation, in the presence or absence of APV. n = 5–7 neurons, *p < 0.05, **p < 0.05, Student's t test.
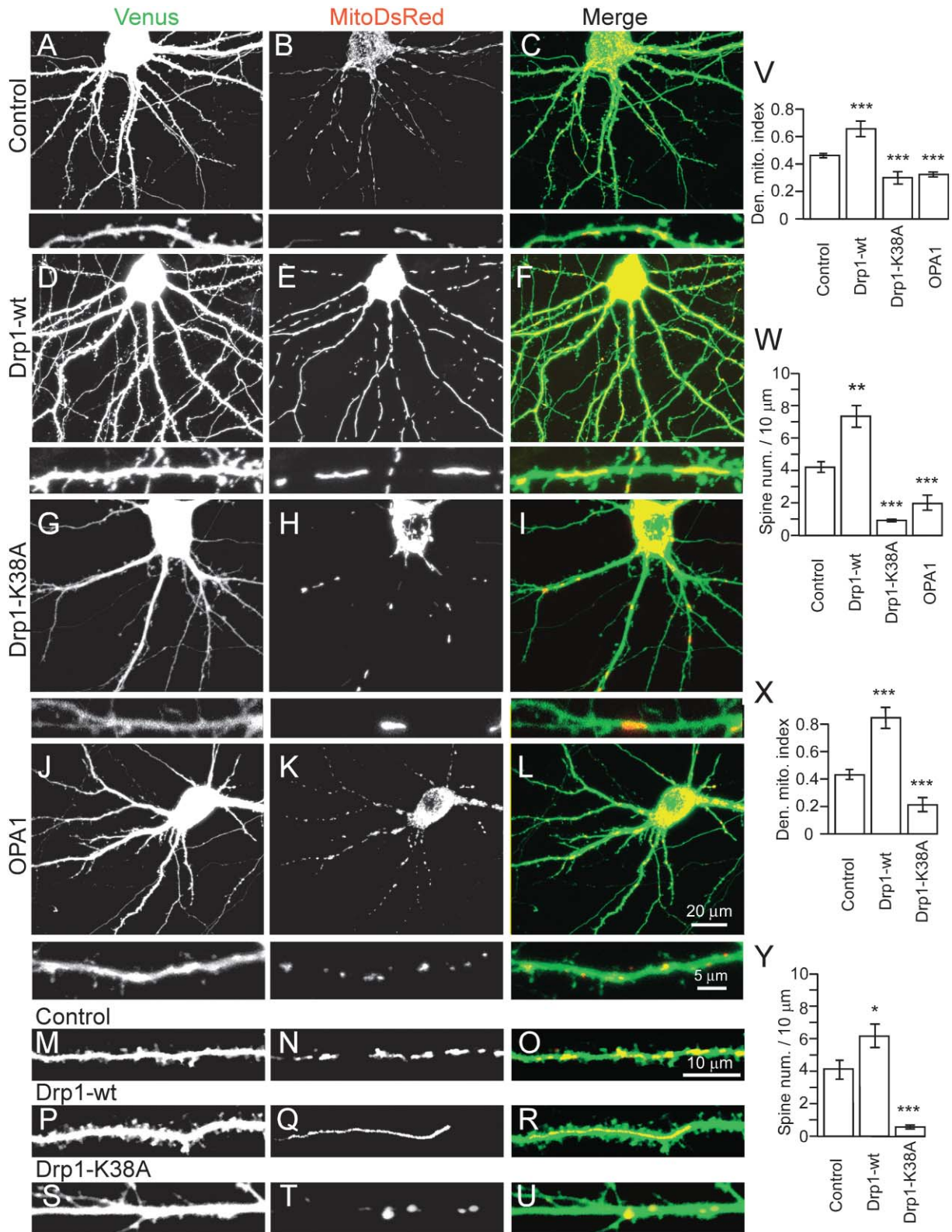
Figure 4. Drp1 and OPA1 Regulate the Distribution of Mitochondria and the Density of Dendritic Spines

(A–L) Div13 neurons were transfected with MitoDsRed and Venus, plus myc-tagged wild-type Drp1 (Drp1-wt), myc-tagged dominant-negative Drp1 (Drp1-K38A), or HA-tagged wild-type OPA1, as indicated, and imaged 4 days later for dendritic morphology (Venus) and mitochondria (MitoDsRed). Each panel shows a representative neuron and a dendritic segment at higher magnification below. (M–U) Cultured hippocampal slices were transfected with GFP and MitoDsRed, plus wild-type Drp1 or Drp1-K38A. Images show segments of apical dendrites of CA1 pyramidal neurons 200–400 μm from the soma. (V–Y) Quantitation of effects of Drp1 and OPA1 on dendritic mitochondrial index (total

to suppress the fusion/fission ratio in Drp1-transfected cells (Figure 7H). The "occlusion" of the depolarization effect by Drp1 overexpression suggests that depolarization reduces the mitochondrial fusion/fission ratio through a Drp1-dependent mechanism. The involvement of Drp1 in activity-regulated mitochondrial fusion/fission is further supported by dominant-negative Drp1 experiments. In neurons expressing Drp1-K38A, the mitochondrial fusion/fission ratio was unresponsive to TTX or KCl (Figures 7I and 7J).

The dendritic mitochondrial index was increased by TTX and decreased by 50 mM KCl (Figure 7C). The reduction of dendritic mitochondrial index by depolarization was blocked by nimodipine and APV. Drp1-K38A also prevented the change of dendritic mitochondrial index induced by TTX or 50 mM KCl. Thus, neuronal activity regulates the motility, fusion/fission balance, and dendritic distribution of mitochondria in a manner at least in part dependent on Drp1 function.

Discussion

In this study, we uncovered a structural and functional interplay between dendritic mitochondria and spines/synapses. First, there was an unexpected physical association between mitochondria and dendritic spines. A small fraction of mitochondria are present within or extend into dendritic protrusions of cultured neurons. This percentage increases in accompaniment with synapse/spine morphogenesis (either developmental or following repetitive depolarization) and in response to local electrical stimulation.

Second, the GTPases that control the distribution of mitochondria in dendrites also regulate the density and plasticity of synapses. Dominant-negative Drp1 or OPA1 overexpression (both of which reduced dendritic mitochondria) led to a decreased density of spines and synapses. Conversely, Drp1 overexpression (which increased dendritic mitochondria) or creatine (which enhanced mitochondrial activity) caused a higher density of spines and synapses. The promoting effects of wild-type Drp1 overexpression or creatine are important, because they imply that the depletion of synapses/spines by dominant-negative Drp1 or OPA1 is unlikely to result from nonspecific cytotoxicity of these GTPase. Remarkably, the ability of neurons to form new excitatory synapses in response to stimulation is also correlated with increased activity of dendritic mitochondria. Thus, mitochondria appear to be limiting factors that determine the ability of dendrites to support synapses and to make new synapses in response to potentiating stimuli. These findings complement recent genetic studies showing the critical importance of presynaptic mitochondria for synaptic transmission (Stowers et al., 2002).

Finally, neuronal activity itself affects the motility, fusion/fission balance, and subcellular distribution of mitochondria in dendrites, depending on calcium influx.

Therefore, mechanisms exist for reciprocal regulation of synapses and mitochondria.

Regulation of Spine and Synapse Density and Plasticity by Dendritic Mitochondria

Mitochondria are rarely observed within dendritic spines in the cortex and hippocampus. Exceptions are the large dendritic spines ("thorny excrescences") of CA3 pyramidal neurons, which frequently contain mitochondria (Adams and Jones, 1982; Cameron et al., 1991; Chicurel and Harris, 1992). The low frequency of dendritic protrusions that contain mitochondria in cultured hippocampal neurons ($<2\%$ at Div18) is compatible with EM studies of the adult brain. Since Div18 cultured neurons are not fully mature or representative of in vivo tissue, the prevalence of mitochondria-positive spines could be even lower in the mature CNS.

Nevertheless, several lines of evidence suggest that the physical encounter of mitochondria with dendritic protrusions is physiologically relevant. First, the number of mitochondria in dendritic protrusions correlates with synapse development. Second, repetitive depolarization that stimulates synapse formation causes the redistribution of mitochondria into dendritic protrusions. Third, focal synaptic stimulation in hippocampal slices induces mitochondria to invade enlarged spines in an NMDA receptor-dependent manner. The functional significance of mitochondria in dendritic protrusions remains to be determined. It might reflect the greater need for ATP and calcium uptake in growing filopodia/spines, analogous to the accumulation of mitochondria in active growth cones of axons (Morris and Hollenbeck, 1993).

The physical interaction of mitochondria and dendritic protrusions during synaptogenesis and spine morphogenesis suggests a local involvement of mitochondria in synapse formation and development. Supporting this idea, we found that Drp1 and OPA1 have large effects on the density of spines/synapses, which were correlated with their effects on dendritic mitochondrial distribution. It is uncertain whether the effects of Drp1 and OPA1 on the density of spines/synapses arise from altered formation or altered stability of synapses. An effect on the formation of synapses is suggested by our time-lapse imaging of synaptogenesis in neurons that are live labeled with PSD-95-Venus. Our finding that Drp1 overexpression increases dendritic mitochondria suggests that the peripheral distribution of mitochondria might be limited by mitochondrial fission, which is believed to depend on Drp1. One possibility is that Drp1 enhances dendritic mitochondrial content by promoting mitochondrial replication, which might require mitochondrial fission (Birky, 2001).

An enhancement of mitochondrial density and activity in dendrites is a simple explanation for the positive effect of Drp1 on synapse number and structural plasticity. In this respect, it is significant that creatine, a stimulator of mitochondrial respiration, can mimic the effect of

---

mitochondrial length/dendrite length) and spine density (number of spines per 10 μm) in dissociated cultured neurons ([V] and [W]; n = 9–21 neurons for each group) and in hippocampal slice cultures ([X] and [Y]; n = 11–22 neurons for each group). Histograms indicate mean $\pm$ SEM. *p $<$ 0.05, **p $<$ 0.01, ***p $<$ 0.001, Student's t test.
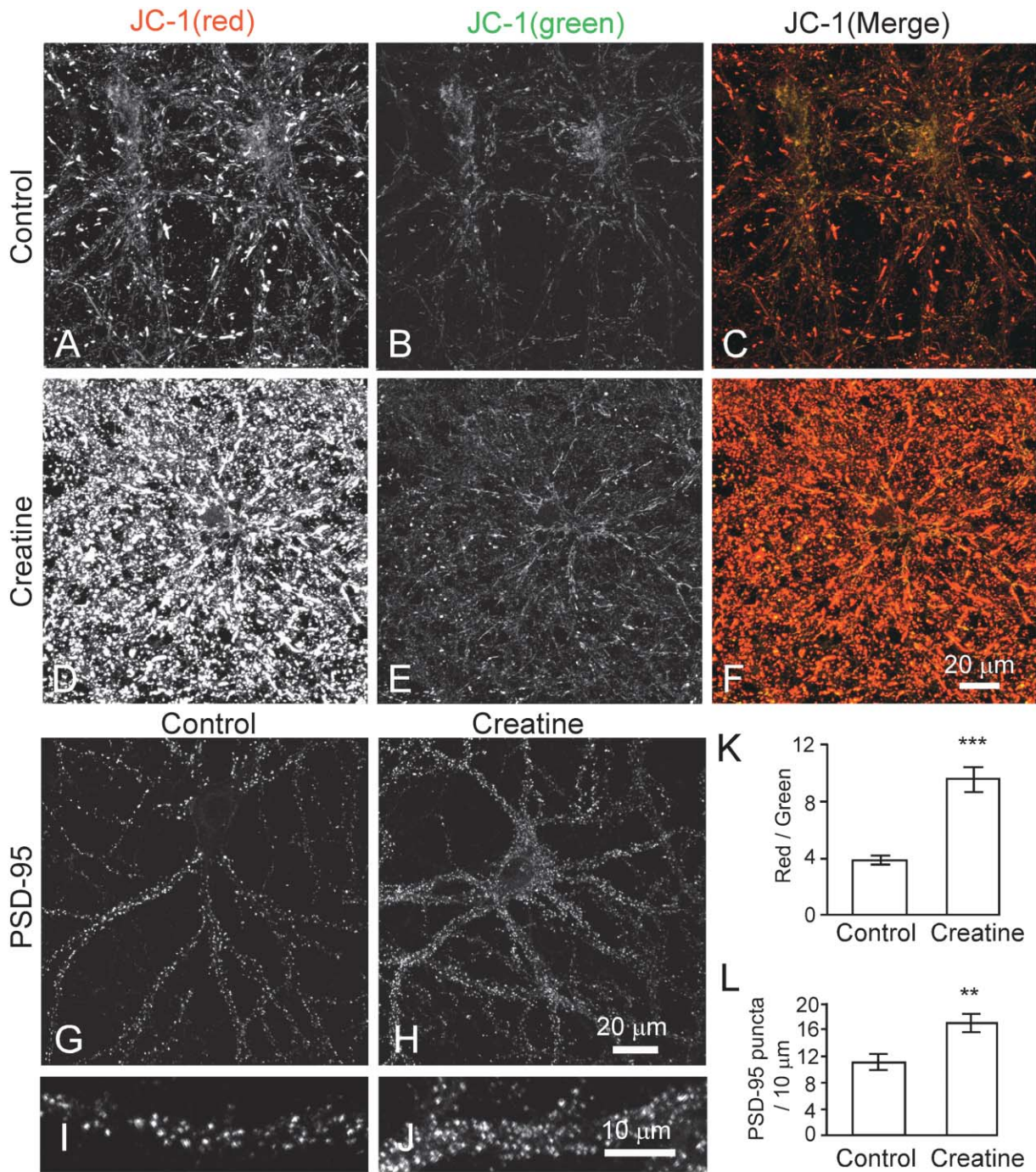
Figure 5. Creatine Enhances Mitochondrial Function and Increases Synapse Density

(A–J) Neurons were treated with 20 mM creatine or untreated (control) for 12 hr and then stained with JC-1 (reporter dye for mitochondrial membrane potential) (A–F) or anti-PSD-95 antibody (G–J).

(K) Creatine boosts mitochondrial membrane potential, as measured by ratio of JC-1 red and green fluorescence.

(L) Creatine increases density of PSD-95 clusters. Histograms indicate mean $\pm$ SEM. n = 15–20 neurons for each group, **p < 0.01, ***p < 0.001, Student's t test.

Drp1 overexpression. Taken together, these pharmacological and molecular genetic data indicate that the level of mitochondrial activity in dendrites may be limiting for synapse density and morphological plasticity.

**Activity-Dependent Regulation
of Dendritic Mitochondria**

Because neurons have long processes and compartment-specific metabolic needs, mitochondria-depen-
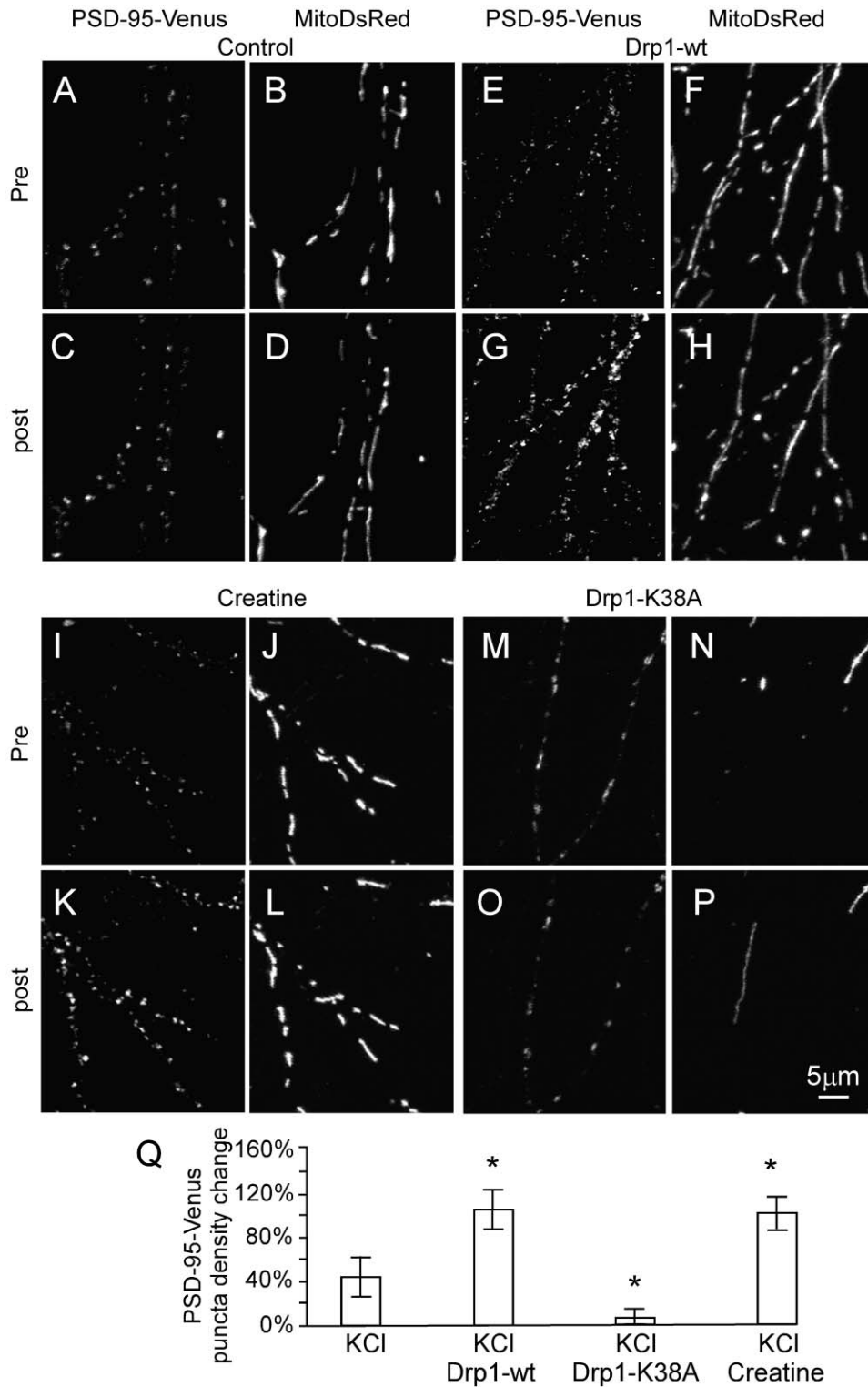
Figure 6. Drp1 and Creatine Promote Activity-Dependent Synaptogenesis

(A–P) Div14 neurons were doubly transfected with PSD-95-Venus and MitoDsRed (A–D, I–L), or were triply transfected with PSD-95-Venus and MitoDsRed, plus Drp1-wt (E-H) or Drp1-K38A (M–P). Three days following transfection, the same neurons were imaged for PSD-95-Venus and MitoDsRed before (pre) and 9 hr after (post) 4 × KCl stimulation. In the experiment using creatine (I–L), 20 mM creatine was included in stimulating solution and the incubation medium following stimulation.

(Q) Effects of wild-type Drp1, Drp1-K38A, and creatine on the percent increase in PSD-95-Venus cluster density induced by 4 × KCl stimulation. Histograms indicate mean ± SEM. n = 9–14 neurons for each group. *p < 0.05, Student's t test.

Figure 7. Regulation of Mitochondrial Dynamics by Neuronal Activity

(A and B) Effect of activity on mitochondrial motility. Two to three days after transfection (Div16-17), mitochondria 20–50 μm away from the soma were selected for time-lapse confocal imaging. Neurons were incubated in Tyrode's solution for 1 hr before collecting images for baseline motility measurement. Cells were then transfered to Tyrode's solution containing 1 μM TTX or 50 mM KCl, and the same mitochondria were imaged again 20 min later. (A) Cumulative frequency plot of speed of mitochondrial movement. TTX accelerated mitochondrial movement, shifting the curve to the right. KCl (50 mM) slowed mitochondrial movement. (B) Mean speed of mitochondrial movement before and after indicated treatments.

(C) Dendritic mitochondrial index before and after indicated treatments. Histograms show mean ± SEM. Each pair of histograms represents the same cells before and after treatment. n = 15–30 mitochondria from 10–15 neurons for each condition. *p < 0.05, **p < 0.01, Student's t test.

(D–J) Effects of Drp1 and activity on mitochondrial fusion/fission. Two to three days after transfection (Div16-17), mitochondria 20–100 μm away from the soma were selected for time-lapse imaging. Neurons were incubated in Tyrode's solution for 1 hr before collecting images for baseline measurement. Cells were then transfered to Tyrode's solution containing 1 μM TTX or 50 mM KCl, and the same mitochondria were imaged again between 10 min and 2 hr after treatment. (D) Effects of transfection of Drp1-wt and Drp1-K38A on mitochondrial fusion/fission ratio. (E and F) Effects of TTX and 50 mM KCl on mitochondrial fusion/fission ratio. (G–J) Effects of TTX and 50 mM KCl on mitochondrial fusion/fission ratio in neurons transfected with Drp1-wt or Drp1-K38A, as indicated. Each line connects mitochondrial fusion/fission ratio of the same neuron before and after treatment. Filled circles represent mean, open squares represent individual cells. Histograms indicate mean ± SEM. n = 8–14 neurons for each group. *p < 0.05, Student's t test.

dent functions cannot depend on diffusion to and from centrally positioned mitochondria. On the contrary, mitochondria have to be appropriately distributed to serve the differential spatial and temporal demands of neurons. Most studies of mitochondrial distribution and transport have been performed in axons of cultured neu-

rons. Although abundant, dendritic mitochondria have been little studied. Overly et al. found that mitochondria were less motile in dendrites than in axons, and, when they moved, the mean excursion length of dendritic mitochondria was shorter (Overly et al., 1996). Recently, stimulation of neurons by excitotoxic doses of glutamate has been shown to inhibit mitochondrial movement and to alter mitochondria from elongated to rounded shape (Rintoul et al., 2003). However, virtually nothing is known about how mitochondrial distribution and movement in dendrites are coordinated with synaptic activity.

Our data indicate that depolarization suppresses the motility of dendritic mitochondria dependent on calcium influx through L-type voltage-gated calcium channels and NMDA receptors. Conversely, reduced neuronal activity speeds up mitochondrial movement. If these effects on motility were localized, then it would be predicted to result in a higher steady-state concentration of mitochondria in active dendritic regions.

Neuronal activity also influences the distribution of mitochondria in dendrites. The mean dendritic mitochondrial index was reduced by global depolarization and elevated by global inhibition of activity. Our finding of reduced dendritic mitochondrial index in depolarized neurons seems at odds with the idea that mitochondria accumulate at active synapses. It should be noted, however, that the dendritic mitochondrial index does not accurately reflect local mitochondrial accumulation at specific synaptic sites, because the index is a ratio that is averaged over relatively long distances of dendrite and is therefore biased toward widespread changes, as opposed to highly localized changes, in mitochondrial density. A second important factor is that only one dimension (length) of mitochondria is measured; therefore, a reduced dendritic mitochondrial index can result from the shortening or aggregation of mitochondria. Indeed, mitochondria tend to round up and cluster when they accumulate subjacent to active spines in response to stimulation (see Figures 2S and 3C for example), and synaptic stimulation causes a shortening of individual mitochondria on average. Thus, it is entirely possible that mitochondria can accumulate underneath an active synapse/spine and yet be associated with a fall in the overall dendritic mitochondrial index within a larger region of the dendrite.

In conclusion, our findings point to a high level of dynamism in dendritic mitochondrial distribution, which is regulated by synaptic activity and correlated with synapse morphogenesis. The kinetic behavior of dendritic mitochondria is in accord with the dynamics of the postsynaptic compartment, in which the turnover of postsynaptic proteins and the mutability of dendritic spines are also controlled by activity (Bonhoeffer and Yuste, 2002; Inoue and Okabe, 2003). Importantly, normal synapse density and activity-dependent synapse formation depend critically on the proper distribution and function of mitochondria in dendrites. Since abnormal mitochondrial morphology and function are associated with neurodegenerative diseases, for example, Alzheimer's diseasae and Parkinson's disease (Castellani et al., 2002; Dawson and Dawson, 2003; Trimmer et al., 2000), our findings raise the possibility that the characteristic synapse loss of such disorders arises in part from mitochondrial dysfunction.

Experimental Procedures

DNA Constructs and Reagents
Myc-tagged Drp1 and Drp1-K38A (from Craig Blackstone) and HA-tagged OPA1 (from Yoshihiro Kubo) were cloned into expression vector pGW1. pDsRed2, pDsRed2-ER, and pEGFP-Endo were from Clontech. The mitochondria targeting sequence from MitoGFP (Clontech) and the Golgi targeting sequence from pECFP-Golgi (Clontech) were ligated to the N terminus of DsRed2 (Clontech). Creatine (Sigma) and JC-1 (Molecular Probes) were purchased.

Neuronal Culture, Transfection, and Immunocytochemistry
Hippocampal neuron cultures were prepared from embryonic day (E) 18–19 rat embryos and immunostained as previously described (Sala et al., 2001). Neurons were plated on coverslips for immunocytochemistry or glass-bottom dishes for time-lapse experiments and transfected with plasmid DNAs using calcium phosphate. Neurons were fixed with 4% formaldehyde, 4% sucrose in PBS (for immunostaining of Drp1/OPA1), or methanol (PSD-95). FM 4-64 staining was performed by stimulating neurons with 40 mM KCl in the presence of 10 μM FM 4-64 (Molecular Probes) for 1 min.

NMDA-Induced GluR2 Internalization
The internalization assay was performed as described (Lee et al., 2002). Briefly, neurons were incubated with a monoclonal antibody against N terminus of GluR2 (Chemicon) to label surface GluR2, then stimulated with 50 μM NMDA for 10 min. Neurons were then fixed, and surface-remaining antibody-labeled GluR2 was saturated by incubation with Cy5 secondary antibody. Neurons were permeabilized with methanol, and internalized GluR2 was stained with Alexa-488 secondary antibody.

Image Acquisition
Images were acquired using a Zeiss inverted LSM510 confocal microscope with 100× (NA 1.4) objective. For time-lapse imaging, glass-bottom dishes were mounted in a chamber incubator at 37°C with 5% CO_2. Confocal images of neurons were collected at 1.5 μm steps through the entire z dimension. To measure mitochondrial or endosome movement, alternate scanning of MitoDsRed/Venus or EndoGFP/DsRed of the same dendritic segment was performed by collecting single optical sections (2 μm) every 3 s for 15 s. For 4 × KCl stimulation, the normal Tyrode's solution was replaced with Tyrode's containing 90 mM KCl (each exposure was 3 min, separated by 10 min recovery in Tyrode's solution). The same neurons were imaged before and at various times after the stimulation using the same confocal settings.

Electrical Stimulation
Organotypic slice cultures of hippocampus were prepared as described (Shi et al., 1999). CA1 pyramidal neurons were transfected by Helios Gene Gun (Bio-Rad). The slice was placed in an imaging chamber and perfused continuously with artificial cerebrospinal fluid gassed with 95% O_2 and 5% CO_2 (Okamoto et al., 2004). The neurons were imaged with a custom-made two-photon laser-scanning microscope with a 60× objective. For electrical stimulation, a glass electrode filled with 1 M NaCl and loaded with fluorescent polystyrene beads (1 μm diameter) at the tip was placed 5–20 μm from the dendrite. The final resistance was ~5 MΩ. Tetanic stimulation (100 Hz, 1 s) was at ~9 V with 200 μs pulse duration. For NMDA receptor blockade, slices were perfused with 100 μM DL-APV during tetanic stimulation. APV was then washed out, and tetanic stimulation was repeated. Only dendrites that showed mitochondrial extension into spines after APV washout were included in the quantification of Figure 3D.

Image Analysis
Confocal images were collapsed to make 2D projections. Spines were counted manually. The length of dendrites and mitochondria was traced and measured with the aid of MetaMorph software (Universal Imaging). All the spines and dendrites in one image frame were measured. To measure the size and intensity of PSD-95 puncta, MetaMorph software was used to 2D deconvolute and threshold the image background. PSD-95 puncta larger than 0.5 μm^2 were

outlined and measured by MetaMorph. Mitochondrial or endosome displacement was measured by using the "track object" macro of MetaMorph. Briefly, a rectangular box was drawn around selected mitochondria/endosomes. The centeroid of a mitochondrion/endosome was determined, and its displacement between adjacent time points was measured. The displacement of the dendritic segment containing the mitochondrion/endosome was similarly measured. The net displacement of mitochondria/endosomes was obtained by subtracting the displacement of the dendritic segment from mitochondrial/endosome displacement. For a given mitochondrion/endosome, six images were taken during a 15 s period, and the five speeds obtained were averaged. Means of mitochondrial/endosome speed under the same treatment were grouped, and statistical analysis was performed using Student's t test. To measure mitochondrial density in the cell body, confocal images were taken with low laser intensity to prevent saturation of MitoDsRed signal. Mitochondria in the cell body was quantified in terms of area occupied. The cumulative mitochondrial area is greater than cell body area due to the overlap of mitochondria. All image analysis was performed "blind" to the treatment conditions.

References

Adams, I., and Jones, D.G. (1982). Quantitative ultrastructural changes in rat cortical synapses during early-, mid- and late-adulthood. Brain Res. 239, 349–363.

Birky, C.W., Jr. (2001). The inheritance of genes in mitochondria and chloroplasts: laws, mechanisms, and models. Annu. Rev. Genet. 35, 125–148.

Bonhoeffer, T., and Yuste, R. (2002). Spine motility. Phenomenology, mechanisms, and function. Neuron 35, 1019–1027.

Cameron, H.A., Kaliszewski, C.K., and Greer, C.A. (1991). Organization of mitochondria in olfactory bulb granule cell dendritic spines. Synapse 8, 107–118.

Castellani, R., Hirai, K., Aliev, G., Drew, K.L., Nunomura, A., Takeda, A., Cash, A.D., Obrenovich, M.E., Perry, G., and Smith, M.A. (2002). Role of mitochondrial dysfunction in Alzheimer's disease. J. Neurosci. Res. 70, 357–360.

Chicurel, M.E., and Harris, K.M. (1992). Three-dimensional analysis of the structure and composition of CA3 branched dendritic spines and their synaptic relationships with mossy fiber boutons in the rat hippocampus. J. Comp. Neurol. 325, 169–182.

Dawson, T.M., and Dawson, V.L. (2003). Molecular pathways of neurodegeneration in Parkinson's disease. Science 302, 819–822.

Delettre, C., Lenaers, G., Pelloquin, L., Belenguer, P., and Hamel, C.P. (2002). OPA1 (Kjer type) dominant optic atrophy: a novel mitochondrial disease. Mol. Genet. Metab. 75, 97–107.

Frank, S., Gaume, B., Bergmann-Leitner, E.S., Leitner, W.W., Robert, E.G., Catez, F., Smith, C.L., and Youle, R.J. (2001). The role of dynamin-related protein 1, a mediator of mitochondrial fission, in apoptosis. Dev. Cell 1, 515–525.

Inoue, A., and Okabe, S. (2003). The dynamic organization of postsynaptic proteins: translocating molecules regulate synaptic function. Curr. Opin. Neurobiol. 13, 332–340.

Karbowski, M., and Youle, R.J. (2003). Dynamics of mitochondrial morphology in healthy cells and during apoptosis. Cell Death Differ. 10, 870–880.

Lee, S.H., Liu, L., Wang, Y.T., and Sheng, M. (2002). Clathrin adaptor AP2 and NSF interact with overlapping sites of GluR2 and play distinct roles in AMPA receptor trafficking and hippocampal LTD. Neuron 36, 661–674.

Matsuzaki, M., Honkura, N., Ellis-Davies, G.C., and Kasai, H. (2004). Structural basis of long-term potentiation in single dendritic spines. Nature 429, 761–766.

Misaka, T., Miyashita, T., and Kubo, Y. (2002). Primary structure of a dynamin-related mouse mitochondrial GTPase and its distribution in brain, subcellular localization, and effect on mitochondrial morphology. J. Biol. Chem. 277, 15834–15842.

Morris, R.L., and Hollenbeck, P.J. (1993). The regulation of bidirectional mitochondrial transport is coordinated with axonal outgrowth. J. Cell Sci. 104, 917–927.

Nagai, T., Ibata, K., Park, E.S., Kubota, M., Mikoshiba, K., and Miyawaki, A. (2002). A variant of yellow fluorescent protein with fast and efficient maturation for cell-biological applications. Nat. Biotechnol. 20, 87–90.

Okamoto, K., Nagai, T., Miyawaki, A., and Hayashi, Y. (2004). Rapid and persistent modulation of actin dynamics regulates postsynaptic reorganization underlying bidirectional plasticity. Nat. Neurosci. 7, 1104–1112.

Olichon, A., Emorine, L.J., Descoins, E., Pelloquin, L., Brichese, L., Gas, N., Guillou, E., Delettre, C., Valette, A., Hamel, C.P., et al. (2002). The human dynamin-related protein OPA1 is anchored to the mitochondrial inner membrane facing the inter-membrane space. FEBS Lett. 523, 171–176.

Olichon, A., Baricault, L., Gas, N., Guillou, E., Valette, A., Belenguer, P., and Lenaers, G. (2003). Loss of OPA1 perturbates the mitochondrial inner membrane structure and integrity, leading to cytochrome c release and apoptosis. J. Biol. Chem. 278, 7743–7746.

Overly, C.C., Rieff, H.I., and Hollenbeck, P.J. (1996). Organelle motility and metabolism in axons vs dendrites of cultured hippocampal neurons. J. Cell Sci. 109, 971–980.

Perkins, G.A., Renken, C.W., Frey, T.G., and Ellisman, M.H. (2001). Membrane architecture of mitochondria in neurons of the central nervous system. J. Neurosci. Res. 66, 857–865.

Pitts, K.R., Yoon, Y., Krueger, E.W., and McNiven, M.A. (1999). The dynamin-like protein DLP1 is essential for normal distribution and morphology of the endoplasmic reticulum and mitochondria in mammalian cells. Mol. Biol. Cell 10, 4403–4417.

Rintoul, G.L., Filiano, A.J., Brocard, J.B., Kress, G.J., and Reynolds, I.J. (2003). Glutamate decreases mitochondrial size and movement in primary forebrain neurons. J. Neurosci. 23, 7881–7888.

Rizzuto, R., Brini, M., Pizzo, P., Murgia, M., and Pozzan, T. (1995). Chimeric green fluorescent protein as a tool for visualizing subcellular organelles in living cells. Curr. Biol. 5, 635–642.

Rowland, K.C., Irby, N.K., and Spirou, G.A. (2000). Specialized synapse-associated structures within the calyx of Held. J. Neurosci. 20, 9135–9144.

Sala, C., Piech, V., Wilson, N.R., Passafaro, M., Liu, G., and Sheng, M. (2001). Regulation of dendritic spine morphology and synaptic function by Shank and Homer. Neuron 31, 115–130.

Shepherd, G.M., and Harris, K.M. (1998). Three-dimensional structure and composition of CA3→CA1 axons in rat hippocampal slices: implications for presynaptic connectivity and compartmentalization. J. Neurosci. 18, 8300–8310.

Shi, S.H., Hayashi, Y., Petralia, R.S., Zaman, S.H., Wenthold, R.J., Svoboda, K., and Malinow, R. (1999). Rapid spine delivery and redistribution of AMPA receptors after synaptic NMDA receptor activation. Science 284, 1811–1816.

Smiley, S.T., Reers, M., Mottola-Hartshorn, C., Lin, M., Chen, A., Smith, T.W., Steele, G.D., Jr., and Chen, L.B. (1991). Intracellular heterogeneity in mitochondrial membrane potentials revealed by a J-aggregate-forming lipophilic cation JC-1. Proc. Natl. Acad. Sci. USA 88, 3671–3675.

Smirnova, E., Shurland, D.L., Ryazantsev, S.N., and van der Bliek, A.M. (1998). A human dynamin-related protein controls the distribution of mitochondria. J. Cell Biol. 143, 351–358.

Smirnova, E., Griparic, L., Shurland, D.L., and van der Bliek, A.M.

(2001). Dynamin-related protein Drp1 is required for mitochondrial division in mammalian cells. Mol. Biol. Cell *12*, 2245–2256.

Stowers, R.S., Megeath, L.J., Gorska-Andrzejak, J., Meinertzhagen, I.A., and Schwarz, T.L. (2002). Axonal transport of mitochondria to synapses depends on Milton, a novel Drosophila protein. Neuron *36*, 1063–1077.

Trimmer, P.A., Swerdlow, R.H., Parks, J.K., Keeney, P., Bennett, J.P., Jr., Miller, S.W., Davis, R.E., and Parker, W.D., Jr. (2000). Abnormal mitochondrial morphology in sporadic Parkinson's and Alzheimer's disease cybrid cell lines. Exp. Neurol. *162*, 37–50.

Walsh, B., Tonkonogi, M., Soderlund, K., Hultman, E., Saks, V., and Sahlin, K. (2001). The role of phosphorylcreatine and creatine in the regulation of mitochondrial respiration in human skeletal muscle. J. Physiol. *537*, 971–978.

Westermann, B. (2002). Merging mitochondria matters: cellular role and molecular machinery of mitochondrial fusion. EMBO Rep. *3*, 527–531.

Wu, G.Y., Deisseroth, K., and Tsien, R.W. (2001). Spaced stimuli stabilize MAPK pathway activation and its effects on dendritic morphology. Nat. Neurosci. *4*, 151–158.

Yaffe, M.P. (1999). The machinery of mitochondrial inheritance and behavior. Science *283*, 1493–1497.

Yoon, Y., and McNiven, M.A. (2001). Mitochondrial division: new partners in membrane pinching. Curr. Biol. *11*, R67–R70.